

000 001 002 003 004 005 006 007 008 009 010 011 012 013 014 015 016 017 018 019 020 021 022 023 024 025 026 027 028 029 030 031 032 033 034 035 036 037 038 039 040 041 042 043 044 045 046 047 048 049 050 051 052 053 MOD-ADAPTER: TUNING-FREE AND VERSATILE MULTI-CONCEPT PERSONALIZATION VIA MODULA- TION ADAPTER

Anonymous authors

Paper under double-blind review

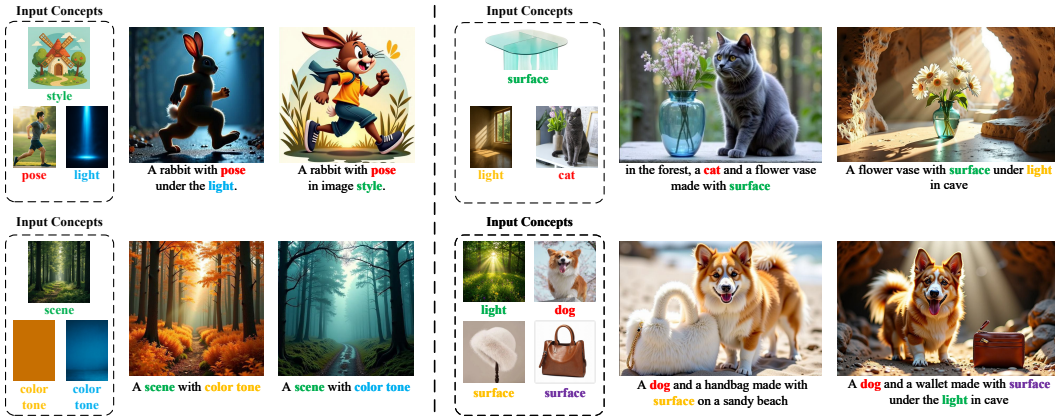


Figure 1: **Results of our multi-concept personalized image generation method.** Our method enables customizing both object and abstract concepts (e.g., pose, light, surface) without test-time fine-tuning. The colored words in the prompt below image indicate concepts to be personalized.

ABSTRACT

Personalized text-to-image generation aims to synthesize images of user-provided concepts in diverse contexts. Despite recent progress in multi-concept personalization, most are limited to object concepts and struggle to customize abstract concepts (e.g., pose, lighting). Some methods have begun exploring multi-concept personalization supporting abstract concepts, but they require test-time fine-tuning for each new concept, which is time-consuming and prone to overfitting on limited training images. In this work, we propose a novel tuning-free method for multi-concept personalization that can effectively customize both object and abstract concepts without test-time fine-tuning. Our method builds upon the modulation mechanism in pre-trained Diffusion Transformers (DiTs) model, leveraging the localized and semantically meaningful properties of the modulation space. Specifically, we propose a novel module, Mod-Adapter, to predict concept-specific modulation direction for the modulation process of concept-related text tokens. It introduces vision-language cross-attention for extracting concept visual features, and Mixture-of-Experts (MoE) layers that adaptively map the concept features into the modulation space. Furthermore, to mitigate the training difficulty caused by the large gap between the concept image space and the modulation space, we introduce a VLM-guided pre-training strategy that leverages the strong image understanding capabilities of vision-language models to provide semantic supervision signals. For a comprehensive comparison, we extend a standard benchmark by incorporating abstract concepts. Our method achieves state-of-the-art performance in multi-concept personalization, supported by quantitative, qualitative, and human evaluations.

054
055
056
057

1 INTRODUCTION

058
059
060
061
062
063
064
065
066
067
Personalized text-to-image generation aims to synthesize images of the concepts specified by user-
provided images in diverse contexts. Recently, this technique has attracted increasing research
attention due to its broad applications, such as poster design and storytelling. However, existing
personalized generation methods primarily focus on object concepts (e.g., common objects and
animals) and struggle to personalize non-object/abstract concepts (e.g., pose and lighting), limiting
their wider applicability. Recently, TokenVerse (Garibi et al., 2025) proposes a multi-concept
personalization framework supporting both object and abstract concepts. However, its concept-
specific test-time fine-tuning paradigm requires fine-tuning for each new concept image at test time,
which is time-consuming and tends to overfit on the single training image, leading to suboptimal
results. In this work, we take the first step toward a tuning-free framework enabling versatile
multi-concept personalization for both objects and abstract concepts as shown in Fig.1.068
069
070
071
072
073
074
075
076
077
078
Existing tuning-free personalized generation methods (Sun et al., 2024; Wang et al., 2025; Huang
et al., 2025; Ma et al., 2024) often face two challenges when customizing abstract concepts. First,
these methods failed to decouple the object concept and abstract concept from the input image due to
the lack of an effective mechanism for extracting abstract features. As a result, they tend to directly
replicate the object into the generated image. For example, when personalizing persons' pose concept,
the generated person often closely resembles the one in the input concept image, rather than merely
reflecting the pose features. This compromises the alignment between the generated image and the
input prompt. Second, the features of abstract concepts are easily influenced by textual features
or other concept features during generation, hindering the accurate preservation of the customized
concept. This issue arises because these methods either concatenate concept image features with text
features, or fuse them through additive cross-attention layers(Ye et al., 2023), resulting in limited
localized control over the generated content.079
080
081
082
083
084
085
086
087
088
089
090
091
092
To address these challenges, we propose a novel tuning-free framework for personalizing multiple
concepts (both objects and abstract concepts) by leveraging the localized and semantically meaningful
properties of the modulation space in DiTs. Specifically, we design a novel module, Mod-Adapter, to
predict modulation directions for customized concepts. The directions are further integrated into the
modulation process of concept-related textual tokens (e.g., "surface"), facilitating disentangled and
localized control over the generated content. To effectively extract the target concept features from the
input image, the Mod-Adapter introduces vision-language cross-attention layers that utilize the CLIP
model's alignment capability between image and textual features. Besides, for accurately mapping
the extracted concept visual features into the direction of DiT modulation space, we introduce a
Mixture-of-Experts (MoE) mechanism within Mod-Adapter, where each expert is responsible for
handling concepts with similar mapping patterns. Furthermore, to mitigate the difficulty of training
Mod-Adapter from scratch due to the large gap between the concept image space and the DiT
modulation space, we propose a VLM-guided pre-training strategy for better initialization, which
leverages the strong image understanding capabilities of vision-language models to provide semantic
supervision signals. To summarize, our key contributions are as follows:093
094
095
096
097
098
099
100
101
102
103
• We propose a novel tuning-free and versatile multi-concept personalization generation method that
can effectively customize both object and abstract concepts, such as pose, lighting, and surface,
without requiring test-time fine-tuning for new concepts.
104
105
106
107
• We propose an innovative module, Mod-Adapter, to predict concept-specific personalized directions
within the modulation space in a novel tuning-free paradigm. Within Mod-Adapter, the designed
vision-language cross-attention extract concept visual features by leveraging the image-text align-
ment capability of CLIP, and the Mixture-of-Experts layers adaptively project these features into the
modulation space. In addition, we propose a novel pre-training strategy guided by a vision-language
model to facilitate training Mod-Adapter.
108
109
110
• We extend the commonly used benchmark by incorporating abstract concepts, resulting in a new
benchmark named DreamBench-Abs. Experimental results demonstrate that our method achieves
state-of-the-art performance in multi-concept personalization generation on this benchmark, as
validated by quantitative and qualitative evaluations as well as user studies.

108
109

2 RELATED WORKS

110
111 In contrast to single-concept personalization works (Tan et al., 2025; Zhang et al., 2025) that can only
112 customize a single concept, our discussion centers on multi-concept personalization, which can be
113 further categorized into tuning-based and tuning-free methods.114
115 **Tuning-Based Multi-concept Personalization.** Tuning-based multi-concept personalization ap-
116 proach (Choi et al., 2025; Jin et al., 2025; Kong et al., 2024; Kwon & Ye, 2025; Gu et al., 2023; Dong
117 et al., 2024; Jiang et al., 2025; Kumari et al., 2023) requires one or more reference images of each
118 concept to fine-tune the model before performing multi-concept personalization at test time. For
119 example, Textual Inversion (Gal et al., 2023) and P+ (Voynov et al., 2023) introduce personalized
120 text-to-image generation by learning a pseudo-word text embedding to represent each input concept.
121 MuDI (Jang et al., 2024) and ConceptGuard (Guo & Jin, 2025) propose solutions to mitigate the
122 concept confusion problem in multi-concept customization, using a form of data augmentation
123 and concept-binding prompts techniques, respectively. Recently, TokenVerse (Garibi et al., 2025)
124 proposed a disentangled multi-concept personalization method, which supports decoupling abstract
125 concepts beyond objects, such as lighting conditions and material surfaces, from images. It optimizes
126 a small MLP for each image to predict the modulation vector offsets for words in the image caption,
127 learning to disentangle concepts of the image. Despite these advancements, tuning-based methods
128 require test-time fine-tuning for unseen concepts, which is time-consuming and prone to overfitting
129 on limited training images, often leading to suboptimal results. Contrasting with TokenVerse, we
propose a novel tuning-free paradigm along with an innovative module, Mod-Adapter, and a novel
pretraining strategy guided by a VLM.130
131 **Tuning-Free Multi-concept Personalization.** Many studies (Sun et al., 2024; Ding et al., 2024; Wu
132 et al., 2024; Huang et al., 2025; Shi et al., 2025; Chen et al., 2025) have attempted to explore tuning-
133 free multi-concept personalized generation, which can generalize to unseen concepts without the need
134 for test-time fine-tuning. Among these, Subject-Diffusion (Ma et al., 2024) and FastComposer (Xiao
135 et al., 2024) integrate subject image features into the text embeddings of subject words. The
136 combined features are then incorporated into the diffusion model through cross-attention layers to
enable personalized generation for multiple subjects. Similarly, λ -ECLIPSE (Patel et al., 2024)
137 projects image-text interleaved features into the latent space of the image generation model using a
138 contrastive pre-training strategy. BLIP-Diffusion (Li et al., 2023a) follows a VLM BLIP-2 (Li et al.,
139 2023b) to pre-train an encoder that produces text-aligned object-type concept representations. In
140 contrast, our pre-training leverages the strong image understanding capabilities of a frozen VLM
141 to facilitate the alignment of concept image features with the DiT modulation space. Benefit
142 from the localized and semantically meaningful properties of the modulation space, our method
143 can effectively customize both object and abstract concepts. Emu2 (Sun et al., 2024) proposes a
144 generative autoregressive multimodal model for various multimodal tasks including multi-concept
145 customization. InstructImagen (Hu et al., 2024a) introduces multimodal instructions and employs
146 multimodal instruction tuning to adapt text-to-image models for customized image generation. MS-
147 Diffusion (Wang et al., 2025) proposes a layout-guided multi-subject personalization framework
148 equipped with a grounding resampler module and a multi-subject cross-attention mechanism. MIP-
149 Adapter (Huang et al., 2025) introduces a weighted-merge mechanism to alleviate the concept
150 confusion problem in multi-concept personalized generation. UniReal (Chen et al., 2025) proposes
151 a unified framework for various image generation tasks, including multi-subject personalization,
152 by learning real-world dynamics from large-scale video data. However, all existing tuning-free
153 multi-concept personalization methods primarily focus on personalizing object concepts, and struggle
to handle customization of abstract concepts. In this study, we propose a novel tuning-free framework
for multi-concept personalization that can effectively customize both object and abstract concepts.154
155
156

3 METHOD

157
158 The overview of our proposed method is shown in Fig. 2. We propose a modulation space adapter
159 module, named Mod-Adapter, for versatile multi-concept customization generation, along with
160 a VLM-supervised adapter pretraining mechanism. In the following sections, we first introduce
161 preliminaries on token modulation in DiTs (Sec. 3.1), and then detail the design of the Mod-Adapter
module (Sec. 3.2) and the proposed pretraining strategy (Sec. 3.3).

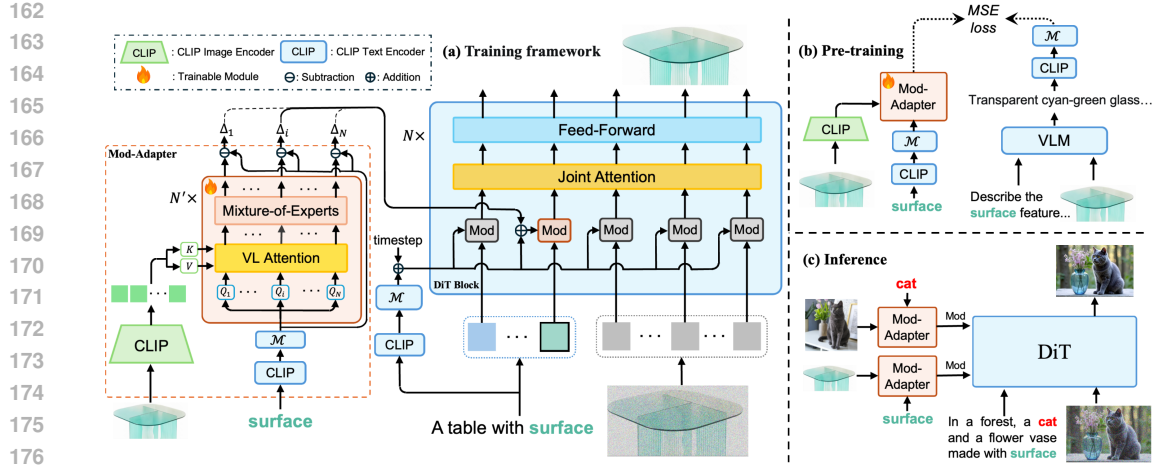


Figure 2: **Overview of the proposed method.** (a) During training, the proposed Mod-Adapter module takes as input a concept image and its corresponding concept word, and predicts a concept-specific modulation direction for each DiT block. The predicted directions are integrated into the modulation (Mod) process of the concept-related text tokens in DiT. (b) Pre-training of the Mod-Adapter module. The concept image is fed into a vision-language model (VLM) to obtain a detailed descriptive caption of the target concept in the image, which is further encoded by a CLIP text encoder and mapped by an MLP layer (\mathcal{M}) into the DiT modulation space. The resulting feature provides the semantic supervision signals for Mod-Adapter. (c) At inference, Mod-Adapter predicts a modulation direction for each customized concept. These directions are integrated into the modulation process of their corresponding text tokens to enable multi-concept customization.

3.1 PRELIMINARIES

Diffusion Transformers(DiT)s (Peebles & Xie, 2023) have recently emerged as a promising architecture for diffusion models (Ho et al., 2020), owing to the strong scalability of transformer (Vaswani et al., 2017). In text-to-image DiTs (Esser et al., 2024; Labs, 2024), text tokens and noisy image tokens are jointly processed through N DiT blocks, each consisting of joint attention and feed-forward layers, to predict the noise added to the image VAE (Kingma & Welling, 2013) latent. In addition, the diffusion timestep condition and a global representation of the text prompt are integrated into the generation process via a token modulation mechanism before joint attention. In this work, we build on FLUX (Labs, 2024), a state-of-the-art DiT-based text-to-image model, for multi-concept personalization. Specifically, in each DiT block, all image and text tokens are modulated by a shared conditioning vector y through Adaptive Layer Normalization (AdaLN) (Peebles & Xie, 2023). The modulation vector y is computed by summing the diffusion timestep embedding t_{emb} and a projection of the CLIP (Radford et al., 2021) pooled prompt embedding, as follows:

$$y = \mathcal{M}_t(t_{emb}) + \mathcal{M}(\text{CLIP}(p)), \quad (1)$$

where p is the text prompt, \mathcal{M}_t and \mathcal{M} are two distinct MLP mapping layers. TokenVerse (Garibi et al., 2025) demonstrates that modulating individual tokens differently enables localized manipulations over the concept of interest during generation process. Specifically, instead of using the same modulation vector for all tokens, the text tokens associated with the target concept are modulated using adjusted modulation vectors:

$$y' = y + s\Delta_{attribute}, \quad (2)$$

where s is a scale factor, the direction $\Delta_{attribute}$ captures the personalized attributes of the concept in the modulation space. The updated vectors y' will induce localized effects on concept-related image regions through the joint attention layers. Thanks to the semantically additive properties of CLIP textual embedding, previous works (Baumann et al., 2025; Hu et al., 2024b; Garibi et al., 2025) have shown that the semantic direction of an attribute can be estimated using contrastive prompts with and without the specific attribute. Specifically, $\Delta_{attribute}$ can be approximated as:

$$\Delta_{attribute} \approx \mathcal{M}(\text{CLIP}(p^+)) - \mathcal{M}(\text{CLIP}(p^0)), \quad (3)$$

216 where p^+ is a positive prompt with some attribute added (e.g., “transparent cyan-green glass surface”),
 217 p^0 is a neutral prompt without attribute (e.g., “surface”), i.e., the concept word itself. Token-
 218 Verse (Garibi et al., 2025) proposes training a separate MLP for each image to predict personalized
 219 directions $\Delta_{attribute}$ for the concept in the image. However, it requires fine-tuning a model at test
 220 time for each new concept image. In contrast, we propose a tuning-free method for multi-concept
 221 customization that can generalize to unseen concepts without test-time fine-tuning, as detailed in the
 222 following sections.

223 3.2 MODULATION SPACE ADAPTER

224 As illustrated in Fig. 2(a), our proposed Mod-Adapter takes a concept image and its corresponding
 225 concept word as input, and predicts a personalized direction $\Delta_{attribute}$ in the modulation space. Since
 226 FLUX (Labs, 2024) contains N DiT blocks, Mod-Adapter predicts a distinct modulation direction
 227 Δ_i for each block to enhance the model’s expressiveness, forming the set $\{\Delta_i \mid i = 1, \dots, N\}$.
 228 As illustrated in Fig. 2(a), in the i -th DiT block, only Δ_i will be added to the original modulation
 229 vector. Inspired by the formulation in Eq. 3, Mod-Adapter first predicts the attribute feature of the
 230 customized concept in the modulation space, denoted as F_i^+ . Then, the personalized modulation
 231 directions $\{\Delta_i \mid i = 1, \dots, N\}$ are computed as follows:

$$232 \Delta_i = F_i^+ - \mathcal{M}(\text{CLIP}(p^0)) \quad (4)$$

233 To obtain attribute feature F_i^+ , the Mod-Adapter is designed with a vision-language cross-attention
 234 mechanism and a Mixture-of-Experts (MoE) component, as detailed below.

235 **Vision Language Cross-Attention.** The proposed Mod-Adapter fully exploits the cross-modal
 236 alignment capability of the CLIP model (Radford et al., 2021) between image and text features.
 237 Specifically, to extract the desired concept features from the input concept image, the corresponding
 238 concept word p^0 (e.g., “surface”) is first passed through the CLIP text encoder followed by the
 239 MLP mapping layer \mathcal{M} to obtain a neutral feature (i.e. $\mathcal{M}(\text{CLIP}(p^0))$). To generate a personalized
 240 modulation direction for each of the N DiT blocks, the neutral feature is further projected by a
 241 linear layer into N queries, denoted as Q_1, \dots, Q_N . Sinusoidal positional embeddings are added
 242 to these queries for distinguishing the direction of different DiT blocks. Meanwhile, we encode
 243 the input concept image using the CLIP image encoder and project the fine-grained features from
 244 the penultimate layer into key and value, denoted as K and V , respectively. Then, cross-attention
 245 between the text and image features is computed using the following formula:

$$246 \text{Attention}(Q_i, K, V) = \text{Softmax}\left(\frac{Q_i K}{\sqrt{d}}\right)V, \quad (5)$$

247 where d is the dimension of key and $i = 1, \dots, N$.

248 **Mixture of Experts.** After extracting the concept visual feature via vision-language cross-attention,
 249 the feature must be mapped into the modulation space of the pre-trained DiT model for effective
 250 integration. A straightforward approach is to use an MLP layer for this mapping. However, we find
 251 that this leads to suboptimal performance, possibly due to the fact that different types of concepts
 252 exhibit distinct mapping patterns. This suggests that concepts with similar mapping patterns should
 253 be handled by the same mapping function, while those with significantly different patterns should
 254 be processed separately. Motivated by this intuition, we introduce a Mixture-of-Experts (MoE)
 255 mechanism to adaptively map various concept visual features into the modulation space, where each
 256 expert corresponds to a distinct MLP mapping network. The core of the MoE lies in the routing
 257 network, which is responsible for assigning different inputs to different experts. A common practice
 258 is to use a learnable linear gating network to perform the routing. However, we find that this approach
 259 tends to suffer from the well-known imbalanced expert utilization problem, where many experts
 260 remain underused during training, even when using a load balancing loss (Shazeer et al., 2017). To
 261 address this issue, we design a simple parameter-free routing mechanism based on the k -means
 262 clustering algorithm. Specifically, we perform k -means clustering over the neutral features of all
 263 concept words (i.e., $\mathcal{M}(\text{CLIP}(p^0))$) in the training dataset, with the number of clusters equal to the
 264 number of experts. Each resulting cluster corresponds to concepts of certain categories, which are
 265 assigned to a specific expert for processing.

266 **Training and Inference.** The training framework of Mod-Adapter is illustrated in Fig. 2(a). The
 267 proposed Mod-Adapter is the only component that requires training, while the pre-trained DiT-based

270 text-to-image generation model is kept frozen. During training, only a single customized concept
 271 condition is added to the modulation space, while at inference time, multiple concept conditions
 272 can be added to the modulation of their corresponding concept tokens to enable multi-concept
 273 personalization, as illustrated in Fig. 2(c). We train Mod-Adapter using the same diffusion objective
 274 as the original DiT model (Labs, 2024). However, we find that training Mod-Adapter from scratch
 275 with this objective alone is challenging, possibly due to the large gap between the modulation space
 276 in DiT and the concept image space. To address this issue, we propose a VLM-supervised pretraining
 277 mechanism for Mod-Adapter to obtain a better initialization, as described below.

279 3.3 MOD-ADAPTER PRE-TRAINING SUPERVISED BY VLM

280 Our proposed pre-training approach is illustrated in Fig. 2(b), and is inspired by the formulations in
 281 Eq. 3 and Eq. 4 from the previous analysis. The attribute feature F_i^+ predicted by Mod-Adapter can be
 282 coarsely supervised during pre-training by the modulation-space representation (i.e., $\mathcal{M}(\text{CLIP}(p^+))$)
 283 of a positive prompt p^+ describing the attribute of the concept in image. To obtain an accurate
 284 positive prompt p^+ of the input concept image, we leverage a pretrained vision-language model
 285 (VLM) that already possesses strong image understanding capabilities. Specifically, the concept
 286 image and a pre-defined system prompt are fed into the VLM, where the system prompt guides the
 287 model to describe the detailed attributes of the target concept in the image, resulting in the output p^+ .
 288 The positive prompt p^+ is then encoded by the CLIP text encoder and mapped by the MLP layer \mathcal{M}
 289 into the modulation space. The resulting feature is used to supervise the Mod-Adapter’s output F_i^+
 290 during pre-training, with the MSE loss defined as:

$$291 \quad \mathcal{L}_{\text{pretrain}} = \frac{1}{N} \sum_{i=1}^N \|F_i^+ - \mathcal{M}(\text{CLIP}(p^+))\|_2^2 \quad (6)$$

294 During pre-training, only the objective $\mathcal{L}_{\text{pretrain}}$ is used, and the output of Mod-Adapter is not
 295 integrated into the memory-intensive DiT model, which enables efficient and lightweight pretraining.
 296 After pretraining, the Mod-Adapter is incorporated into the DiT model and trained further using only
 297 the diffusion objective mentioned above.

300 4 EXPERIMENTS

301 4.1 EXPERIMENTAL SETUPS

303 **Datasets.** We train our model using the open-source MVImgNet object dataset (Yu et al., 2023),
 304 the Animal Faces-HQ (AFHQ) dataset (Choi et al., 2020), and synthetic data generated by the
 305 FLUX (Labs, 2024) model. MVImgNet contains multi-view images of real-world objects. We
 306 select objects of 40 commonly seen categories from it and use a single-view image per object for
 307 training. AFHQ is a high-quality animal face dataset containing common categories such as cats,
 308 dogs, and wildlife. For abstract concepts, we synthesize training data using the FLUX model, which
 309 has been demonstrated by recent works (Tan et al., 2024; Cai et al., 2025) to be an effective diffusion
 310 self-distillation strategy. The resulting abstract concept dataset covers a range of common categories,
 311 including those used in TokenVerse (Garibi et al., 2025) (environment light, human pose, scene, and
 312 surface), as well as our additional extensions of image style and color tone. In total, our final training
 313 dataset contains 106,104 images paired with corresponding captions.

314 **Implementation Details.** We adopt the pre-trained FLUX.1-dev model as our DiT backbone
 315 containing $N = 57$ blocks. The Mod-Adapter contains $N' = 4$ blocks and the number of experts
 316 is set to 12 according to the ablation study. It is the only module that requires optimization during
 317 training, with a total parameter count of just 1,667.77M. For more details, please see Appendix C.

318 **Comparison Methods.** We compare our method with state-of-the-art multi-subject personalization
 319 approaches, including tuning-free methods Emu2 (Sun et al., 2024), MIP-Adapter (Huang et al.,
 320 2025), and MS-Diffusion (Wang et al., 2025), as well as the tuning-based method TokenVerse (Garibi
 321 et al., 2025). Since the training datasets used by MIP-Adapter and MS-Diffusion do not include
 322 abstract concept data, we fine-tune their released model weights using our abstract concept data
 323 to ensure a fair comparison. Emu2 has not released its training code, but its training data includes
 common abstract concepts such as style and lighting.

324
 325
 326
 Table 1: **Quantitative comparison.** CP and PF score evaluates concept preservation and image-text
 alignment respectively. Their product CP·PF is a comprehensive evaluation score. CLIP-T evaluates
 the image-text alignment. All scores range from 0 to 1. \uparrow : higher is better.

327 328 Methods	329 Multi-Concept				329 Single-Concept			
	330 CP \uparrow	330 PF \uparrow	330 CP·PF \uparrow	330 CLIP-T \uparrow	331 CP \uparrow	331 PF \uparrow	331 CP·PF \uparrow	331 CLIP-T \uparrow
Emu2 (Sun et al., 2024)	0.53	0.48	0.25	0.299	0.73	0.57	0.42	0.288
MIP-Adapter (Huang et al., 2025)	0.68	0.55	0.37	0.328	0.70	0.39	0.27	0.277
MS-Diffusion (Wang et al., 2025)	0.62	0.51	0.32	0.326	0.57	0.40	0.23	0.282
TokenVerse (Garibi et al., 2025)	0.56	0.56	0.31	0.316	0.58	0.66	0.38	0.312
Mod-Adapter(Ours)	0.70	0.89	0.62	0.330	0.61	0.89	0.54	0.315

333
 334
 335
 336
 337
 338
 339
 340
Evaluation Benchmarks. Following prior work (Wang et al., 2025; Huang et al., 2025; Sun et al.,
 341
 342
 343
 344
 345
 346
 347
 348
 349
 350
 2024), we evaluate the performance of both single-concept and multi-concept personalization on the
 DreamBench benchmark (Ruiz et al., 2023), which contains 30 object or animal concepts and 25
 template prompts. In addition, we extend the DreamBench by incorporating 20 abstract concepts
 for a more comprehensive evaluation, resulting in a new benchmark named DreamBench-Abs. For
 multi-concept evaluation, we follow TokenVerse (Garibi et al., 2025) to construct 30 combinations
 from all 50 concepts. None of the test images or prompts appear in our training set. Among all
 methods, only TokenVerse, based on per-sample training, requires using the test images for training.

351
 352
 353
 354
 355
 356
 357
 358
 359
 360
 361
 362
 363
 364
Metrics. We follow prior methods (Wang et al., 2025; Huang et al., 2025; Sun et al., 2024; Garibi
 365
 366
 367
 368
 369
 370
 371
 372
 373
 374
 375
 376
 377
 et al., 2025) to evaluate both single-concept and multi-concept personalization from two perspectives:
 the fidelity of the generated concepts (Concept Preservation) and the alignment between the generated
 images and the textual prompt (Prompt Fidelity). As our task involves both object and abstract
 concepts, we follow TokenVerse (Garibi et al., 2025) and adopt a multimodal LLM-based (OpenAI,
 2024; Peng et al., 2025) scoring approach. For each generated image, the multimodal LLM outputs a
 Concept Preservation (**CP**) and a Prompt Fidelity (**PF**) score, which evaluate concept preservation
 and image-text alignment, respectively. Since there is often a trade-off between the two metrics, their
 product (**CP·PF**) is also reported as a comprehensive score (Peng et al., 2025). Besides, we evaluate
 image-text alignment by measuring the similarity between their CLIP embeddings (**CLIP-T**).

4.2 COMPARISONS

353
 354
 355
 356
 357
 358
 359
 360
 361
 362
 363
 364
Quantitative Comparison. We report the quantitative comparison results in Tab. 1. In multi-concept
 personalization, our method outperforms all previous approaches across all metrics. Specifically, it
 achieves the highest CP·PF score of 0.62, demonstrating a substantial +67.6% improvement over the
 second-best method, MIP-Adapter (0.37). While MIP-Adapter and MS-Diffusion achieve competitive
 CP scores (0.68 and 0.62, respectively), their PF scores (0.55 and 0.51) are significantly lower
 than ours (0.89). Consistent with observations from prior work, the CLIP-T metric is insensitive
 to variations in image-text alignment, with all methods scoring around 0.3. In single-concept
 personalization, our method still achieves significantly higher performance on the combined metric
 CP·PF compared to all other methods. Although Emu2 and MIP-Adapter outperform us on the
 CP metric, they perform significantly worse on both PF and CLIP-T, indicating that they sacrifice
 prompt fidelity to achieve higher concept preservation. In addition, while Emu2 performs well in
 single-concept personalization, its performance drops notably in the multi-concept setting.

365
 366
 367
 368
 369
 370
 371
 372
 373
 374
 375
 376
 377
Qualitative Comparison. Fig. 3 presents representative qualitative comparisons between our method
 and other approaches. In the first row of single-concept personalization, our method successfully
 generates a wallet with a brown leather surface consistent with the input concept image. In contrast,
 MS-Diffusion, MIP-Adapter, and Emu2 fail to effectively disentangle the abstract concept 'brown
 leather' from the object (handbag). As a result, they simply replicate the original object in the
 generated image, producing an undesired brown leather handbag instead of the desired wallet. This
 observation aligns with their high CP scores but low PF scores in Tab. 1. In the multi-subject per-
 sonalization setting, our method continues to demonstrate superior concept preservation and prompt
 alignment performance, whereas Emu2 shows reduced effectiveness, often generating unnatural
 concept combinations. MS-Diffusion and MIP-Adapter are still prone to "copy-paste" artifacts (e.g.,
 the glass table in the second row and the man in the third row), which negatively affect prompt
 alignment. Meanwhile, their concept preservation performance also declines. In both single- and
 multi-concept personalization settings, tuning-based methods TokenVerse tend to overfit due to the
 need for fine-tuning on each input concept image, which compromises both concept preservation and
 prompt alignment. Its per-sample training paradigm only encourages the model to better reconstruct

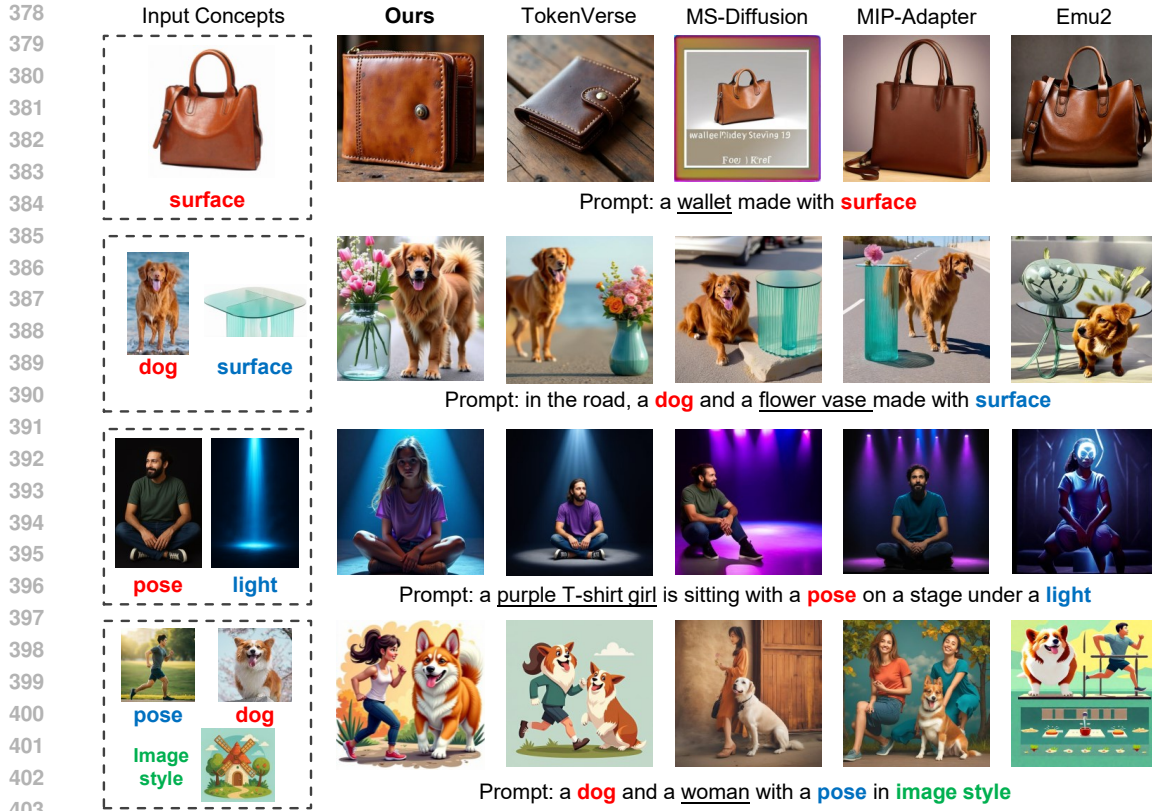


Figure 3: **Qualitative comparison.** The left dashed box shows input concept images. Colored words in the prompt indicate concepts to be personalized, while underlined text highlights elements that reflect differences in prompt alignment performance between methods.

Table 2: **User study results.** CP and PF respectively record the average scores given by volunteers for concept preservation and image-text alignment. Scores range from 1 to 5. \uparrow : higher is better.

Methods	Multi-Concept		Single-Concept	
	CP \uparrow	PF \uparrow	CP \uparrow	PF \uparrow
Emu2 (Sun et al., 2024)	2.10	2.02	2.66	3.04
MIP-Adapter (Huang et al., 2025)	2.83	2.78	2.53	2.14
MS-Diffusion (Wang et al., 2025)	3.16	3.14	2.42	2.60
TokenVerse (Garibi et al., 2025)	3.35	3.48	3.43	2.87
Mod-Adapter(Ours)	4.29	4.40	4.49	4.60

the training images with the input of corresponding image captions, but it does not ensure good performance on unseen test prompts in real-world scenarios. All these results demonstrate the superior performance of our method in multi-concept personalized generation.

User Study. Following the evaluation setting of TokenVerse (Garibi et al., 2025), we conducted a user study with 32 participants, asking them to rate each generated image in terms of concept preservation (CP) and prompt fidelity (PF). Each participant evaluated five results per method on both single- and multi-concept personalization settings, resulting in 4000 votes. The results are reported in Tab. 2. Our method receives consistently higher user ratings than all compared methods in both CP and PF. For more details about the user study, please see Appendix D.

4.3 ABLATION STUDY

Mod-Adapter Pre-training. We design an ablation variant excluding the Mod-Adapter pre-training strategy. Specifically, we train the Mod-Adapter from scratch using only the diffusion objective, under the same training settings and for the same total number of steps (176K) as the full model. The quantitative results of this variant are shown in the “w/o Pre-training” row of Tab. 3. Both CP and PF scores drop significantly for both single-concept and multi-concept personalization. Furthermore, as illustrated in the “w/o pre-training” column of Fig. 4, the generation quality degrades in terms of both concept preservation and prompt fidelity compared to our full model. This degradation is due to



Figure 4: **Qualitative ablation results.** The left dashed box shows input concept images. Eliminating any proposed component degrades qualitative performance.

Table 3: **Quantitative ablation results.**

Methods	Multi-Concept				Single-Concept			
	CP↑	PF↑	CP-PF↑	CLIP-T↑	CP↑	PF↑	CP-PF↑	CLIP-T↑
w/o k-means routing	0.59	0.83	0.49	0.324	0.54	0.82	0.44	0.311
w/o MoE	0.52	0.68	0.35	0.313	0.51	0.82	0.42	0.311
w/o VL-attn	0.52	0.75	0.39	0.329	0.57	0.86	0.49	0.317
w/o pre-training	0.29	0.58	0.17	0.306	0.33	0.72	0.24	0.308
Mod-Adapter(Ours)	0.70	0.89	0.62	0.330	0.61	0.89	0.54	0.315

the large gap between the modulation space in DiT and the concept image space. In contrast, our proposed VLM-supervised pre-training mechanism effectively mitigates this training difficulty by leveraging the strong understanding capabilities of the VLM to provide an initialization.

Vision Language Cross-Attention. We design an ablation variant removing VL cross-attention from the Mod-Adapter module. In this variant, the concept word is not used as input, and the VL-attention is replaced with a standard cross-attention layer, where the queries are N learnable query tokens following MS-Diffusion (Wang et al., 2025). As shown in the “w/o VL-atten” results in Tab. 3 and Fig. 4, this variant shows slightly degraded performance in both concept preservation and prompt fidelity in single-concept personalization. However, in the multi-concept setting, the performance drop is more significant, possibly due to the learnable query mechanism’s inability to effectively extract target concept features. As mentioned earlier, the CLIP-T metric is insensitive to variations in prompt alignment; thus, the CLIP-T score of this variant remains comparable to, or even slightly higher than that of our full model.

Mixture of Experts. We design an ablation variant by replacing the MoE layer with a single MLP, while keeping the overall parameter count of the Mod-Adapter unchanged. As shown in the “w/o MoE” results on Tab. 3 and Fig. 4, this variant performs worse than our full model in both concept preservation and prompt fidelity. This is because a simple MLP is insufficient to accurately project diverse concept features into the modulation space of the pre-trained DiT network. For more ablation analysis on the number of experts, please refer to the Appendix F.

K-means MoE Routing. We design a variant following the common practice of using a learnable linear gating network for routing. As shown in Tab. 3 and Fig. 4, compared to our full model, this variant shows degraded performance in both concept preservation and prompt fidelity, but it still performs better than the “w/o MoE” variant. This is because the learnable linear gating network tends to result in the under-utilization of certain experts, which is equivalent to using fewer experts than our full model. For more detailed analysis and the ablation on the clustering method, please refer to the Appendix F.

5 CONCLUSION

We propose a novel tuning-free framework for versatile multi-concept personalization, capable of customizing both object and abstract concepts without test-time fine-tuning. Our method contains a

486 novel module, Mod-Adapter, consisting of vision-language cross-attention layers for concept visual
 487 feature extraction and Mixture-of-Experts layers for projecting features into the modulation space.
 488 Additionally, we introduce an innovative VLM-guided pretraining strategy to facilitate Mod-Adapter
 489 training. We conduct extensive experiments and demonstrate the superiority and effectiveness of our
 490 proposed method. For the limitation discussion of our method, please refer to the Appendix A.
 491

492 REFERENCES

494 Stefan Andreas Baumann, Felix Krause, Michael Neumayr, Nick Stracke, Melvin Sevi, Vincent Tao
 495 Hu, and Björn Ommer. Continuous, Subject-Specific Attribute Control in T2I Models by Identify-
 496 ing Semantic Directions. In *CVPR*, 2025.

497 Shengqu Cai, Eric Chan, Yunzhi Zhang, Leonidas Guibas, Jiajun Wu, and Gordon. Wetzstein.
 498 Diffusion self-distillation for zero-shot customized image generation. In *CVPR*, 2025.

499 Xi Chen, Zhifei Zhang, He Zhang, Yuqian Zhou, Soo Ye Kim, Qing Liu, Yijun Li, Jianming Zhang,
 500 Nanxuan Zhao, Yilin Wang, et al. UniReal: Universal image generation and editing via learning
 501 real-world dynamics. In *CVPR*, 2025.

503 Yongjin Choi, Chanhun Park, and Seung Jun Baek. DynASyn: Multi-subject personalization enabling
 504 dynamic action synthesis. In *AAAI*, volume 39, pp. 2564–2572, 2025.

505 Yunjey Choi, Youngjung Uh, Jaejun Yoo, and Jung-Woo Ha. StarGAN v2: Diverse image synthesis
 506 for multiple domains. In *CVPR*, pp. 8188–8197, 2020.

508 Ganggui Ding, Canyu Zhao, Wen Wang, Zhen Yang, Zide Liu, Hao Chen, and Chunhua Shen.
 509 FreeCustom: Tuning-free customized image generation for multi-concept composition. In *CVPR*,
 510 pp. 9089–9098, 2024.

511 Jiahua Dong, Wenqi Liang, Hongliu Li, Duzhen Zhang, Meng Cao, Henghui Ding, Salman H Khan,
 512 and Fahad Shahbaz Khan. How to continually adapt text-to-image diffusion models for flexible
 513 customization? *Advances in Neural Information Processing Systems*, 37:130057–130083, 2024.

515 Patrick Esser, Sumith Kulal, Andreas Blattmann, Rahim Entezari, Jonas Müller, Harry Saini, Yam
 516 Levi, Dominik Lorenz, Axel Sauer, Frederic Boesel, et al. Scaling rectified flow transformers for
 517 high-resolution image synthesis. In *ICML*, 2024.

518 Rinon Gal, Yuval Alaluf, Yuval Atzmon, Or Patashnik, Amit Haim Bermano, Gal Chechik, and
 519 Daniel Cohen-or. An image is worth one word: Personalizing text-to-image generation using
 520 textual inversion. In *ICLR*, 2023.

522 Daniel Garibi, Shahar Yadin, Roni Paiss, Omer Tov, Shiran Zada, Ariel Ephrat, Tomer Michaeli, Inbar
 523 Mosseri, and Tali Dekel. TokenVerse: Versatile multi-concept personalization in token modulation
 524 space. *ACM SIGGRAPH 2025*, 2025.

525 Yuchao Gu, Xintao Wang, Jay Zhangjie Wu, Yujun Shi, Yunpeng Chen, Zihan Fan, Wuyou Xiao,
 526 Rui Zhao, Shuning Chang, Weijia Wu, et al. Mix-of-show: Decentralized low-rank adaptation for
 527 multi-concept customization of diffusion models. *Advances in Neural Information Processing
 528 Systems*, 36:15890–15902, 2023.

529 Zirun Guo and Tao Jin. ConceptGuard: Continual personalized text-to-image generation with
 530 forgetting and confusion mitigation. In *CVPR*, 2025.

532 Jonathan Ho, Ajay Jain, and Pieter Abbeel. Denoising diffusion probabilistic models. *NeurIPS*, 33:
 533 6840–6851, 2020.

534 Hexiang Hu, Kelvin C.K. Chan, Yu-Chuan Su, Wenhui Chen, Yandong Li, Kihyuk Sohn, Yang Zhao,
 535 Xue Ben, Boqing Gong, William Cohen, Ming-Wei Chang, and Xuhui Jia. Instruct-Imagen: Image
 536 generation with multi-modal instruction. In *CVPR*, pp. 4754–4763, June 2024a.

538 Taihang Hu, Linxuan Li, Joost van de Weijer, Hongcheng Gao, Fahad Shahbaz Khan, Jian Yang,
 539 Ming-Ming Cheng, Kai Wang, and Yaxing Wang. Token merging for training-free semantic
 540 binding in text-to-image synthesis. *NeurIPS*, 37:137646–137672, 2024b.

540 Qihan Huang, Siming Fu, Jinlong Liu, Hao Jiang, Yipeng Yu, and Jie Song. Resolving multi-condition
 541 confusion for finetuning-free personalized image generation. In *AAAI*, volume 39, pp. 3707–3714,
 542 2025.

543 Sangwon Jang, Jaehyeong Jo, Kimin Lee, and Sung Ju Hwang. Identity decoupling for multi-subject
 544 personalization of text-to-image models. In *NeurIPS*, 2024.

545 Jiaxiu Jiang, Yabo Zhang, Kailai Feng, Xiaohe Wu, Wenbo Li, Renjing Pei, Fan Li, and Wangmeng
 546 Zuo. Mc^2 : Multi-concept guidance for customized multi-concept generation. In *Proceedings of
 547 the Computer Vision and Pattern Recognition Conference*, pp. 2802–2812, 2025.

548 Jian Jin, Yu Zhenbo, Shen Yang, Zhenyong Fu, and Jian Yang. LatexBlend: Scaling multi-concept
 549 customized generation with latent textual blending. In *CVPR*, 2025.

550 Diederik P Kingma and Jimmy Ba. Adam: A method for stochastic optimization. *arXiv preprint
 551 arXiv:1412.6980*, 2014.

552 Diederik P Kingma and Max Welling. Auto-encoding variational bayes. *arXiv e-prints*, pp. arXiv–
 553 1312, 2013.

554 Zhe Kong, Yong Zhang, Tianyu Yang, Tao Wang, Kaihao Zhang, Bizhu Wu, Guanying Chen, Wei Liu,
 555 and Wenhan Luo. OMG: Occlusion-friendly personalized multi-concept generation in diffusion
 556 models. In *ECCV*, pp. 253–270. Springer, 2024.

557 Nupur Kumari, Bingliang Zhang, Richard Zhang, Eli Shechtman, and Jun-Yan Zhu. Multi-concept
 558 customization of text-to-image diffusion. In *CVPR*, pp. 1931–1941, 2023.

559 Gihyun Kwon and Jong Chul Ye. TweedieMix: Improving multi-concept fusion for diffusion-based
 560 image/video generation. In <https://arxiv.org/abs/2410.05591>, 2025.

561 Black Forest Labs. Flux. <https://github.com/black-forest-labs/flux>, 2024.

562 Dongxu Li, Junnan Li, and Steven Hoi. Blip-diffusion: Pre-trained subject representation for
 563 controllable text-to-image generation and editing. *Advances in Neural Information Processing
 564 Systems*, 36:30146–30166, 2023a.

565 Junnan Li, Dongxu Li, Silvio Savarese, and Steven Hoi. Blip-2: Bootstrapping language-image
 566 pre-training with frozen image encoders and large language models. In *International conference
 567 on machine learning*, pp. 19730–19742. PMLR, 2023b.

568 Ming Li, Taojiannan Yang, Huafeng Kuang, Jie Wu, Zhaoning Wang, Xuefeng Xiao, and Chen Chen.
 569 ControlNet++: Improving conditional controls with efficient consistency feedback: Project page:
 570 liming-ai.github.io/controlnet_plus_plus. In *ECCV*, pp. 129–147. Springer, 2024.

571 Jian Ma, Junhao Liang, Chen Chen, and Haonan Lu. Subject-Diffusion: Open domain personalized
 572 text-to-image generation without test-time fine-tuning. In *ACM SIGGRAPH 2024 Conference
 573 Papers*, pp. 1–12, 2024.

574 Chong Mou, Xintao Wang, Liangbin Xie, Yanze Wu, Jian Zhang, Zhongang Qi, and Ying Shan.
 575 T2I-Adapter: Learning adapters to dig out more controllable ability for text-to-image diffusion
 576 models. In *AAAI*, volume 38, pp. 4296–4304, 2024.

577 OpenAI. Introducing gpt-4o and more tools to chatgpt free users. 2024. URL <https://openai.com/index/gpt-4o-and-more-tools-to-chatgpt-free/>.

578 Maitreya Patel, Sangmin Jung, Chitta Baral, and Yezhou Yang. λ -ECLIPSE: Multi-concept personal-
 579 ized text-to-image diffusion models by leveraging clip latent space. *TMLR*, 2024.

580 William Peebles and Saining Xie. Scalable diffusion models with transformers. In *ICCV*, pp.
 581 4195–4205, 2023.

582 Yuang Peng, Yuxin Cui, Haomiao Tang, Zekun Qi, Runpei Dong, Jing Bai, Chunrui Han, Zheng
 583 Ge, Xiangyu Zhang, and Shu-Tao Xia. DreamBench++: A human-aligned benchmark for person-
 584 alized image generation. In *ICLR*, 2025. URL <https://openreview.net/forum?id=4GSOESJrk6>.

594 Alec Radford, Jong Wook Kim, Chris Hallacy, Aditya Ramesh, Gabriel Goh, Sandhini Agarwal,
 595 Girish Sastry, Amanda Askell, Pamela Mishkin, Jack Clark, et al. Learning transferable visual
 596 models from natural language supervision. In *ICML*, pp. 8748–8763. PMLR, PMLR, 2021.

597

598 Nataniel Ruiz, Yuanzhen Li, Varun Jampani, Yael Pritch, Michael Rubinstein, and Kfir Aberman.
 599 DreamBooth: Fine tuning text-to-image diffusion models for subject-driven generation. In *CVPR*,
 600 pp. 22500–22510, 2023.

601

602 Noam Shazeer, Azalia Mirhoseini, Krzysztof Maziarz, Andy Davis, Quoc Le, Geoffrey Hinton, and
 603 Jeff Dean. Outrageously large neural networks: The sparsely-gated mixture-of-experts layer. *arXiv*
 604 preprint *arXiv:1701.06538*, 2017.

605

606 Qingyu Shi, Lu Qi, Jianzong Wu, Jinbin Bai, Jingbo Wang, Yunhai Tong, and Xiangtai Li. DreamRe-
 607 lation: Bridging customization and relation generaion. In *CVPR*, 2025.

608

609 Quan Sun, Yufeng Cui, Xiaosong Zhang, Fan Zhang, Qiying Yu, Yueze Wang, Yongming Rao,
 610 Jingjing Liu, Tiejun Huang, and Xinlong Wang. Generative multimodal models are in-context
 611 learners. In *CVPR*, pp. 14398–14409, 2024.

612

613 Zhenxiong Tan, Songhua Liu, Xingyi Yang, Qiaochu Xue, and Xinchao Wang. OminiControl:
 614 Minimal and universal control for diffusion transformer. *arXiv preprint arXiv:2411.15098*, 2024.

615

616 Zhenxiong Tan, Songhua Liu, Xingyi Yang, Qiaochu Xue, and Xinchao Wang. Ominicontrol:
 617 Minimal and universal control for diffusion transformer. 2025.

618

619 Ashish Vaswani, Noam Shazeer, Niki Parmar, Jakob Uszkoreit, Llion Jones, Aidan N Gomez, Łukasz
 620 Kaiser, and Illia Polosukhin. Attention is all you need. *NeurIPS*, 30, 2017.

621

622 Andrey Voynov, Qinghao Chu, Daniel Cohen-Or, and Kfir Aberman. p+: Extended textual condition-
 623 ing in text-to-image generation. *arXiv preprint arXiv:2303.09522*, 2023.

624

625 Xierui Wang, Siming Fu, Qihan Huang, Wanggui He, and Hao Jiang. MS-Diffusion: Multi-subject
 626 zero-shot image personalization with layout guidance. In *ICLR*, 2025.

627

628 Zhi-Fan Wu, Lianghua Huang, Wei Wang, Yanheng Wei, and Yu Liu. MultiGen: Zero-shot image
 629 generation from multi-modal prompts. In *ECCV*, pp. 297–313. Springer, 2024.

630

631 Guangxuan Xiao, Tianwei Yin, William T Freeman, Frédo Durand, and Song Han. FastComposer:
 632 Tuning-free multi-subject image generation with localized attention. *IJCV*, pp. 1–20, 2024.

633

634 Hu Ye, Jun Zhang, Sibo Liu, Xiao Han, and Wei Yang. IP-Adapter: Text compatible image prompt
 635 adapter for text-to-image diffusion models. *arXiv preprint arXiv:2308.06721*, 2023.

636

637 Xianggang Yu, Mutian Xu, Yidan Zhang, Haolin Liu, Chongjie Ye, Yushuang Wu, Zizheng Yan,
 638 Tianyou Liang, Guanying Chen, Shuguang Cui, and Xiaoguang Han. MVIImgNet: A large-scale
 639 dataset of multi-view images. In *CVPR*, 2023.

640

641 Lvmin Zhang, Anyi Rao, and Maneesh Agrawala. Adding conditional control to text-to-image
 642 diffusion models. In *ICCV*, pp. 3836–3847, 2023.

643

644 Yuxuan Zhang, Yirui Yuan, Yiren Song, Haofan Wang, and Jiaming Liu. Easycontrol: Adding
 645 efficient and flexible control for diffusion transformer. *arXiv preprint arXiv:2503.07027*, 2025.

646

647 Shihao Zhao, Dongdong Chen, Yen-Chun Chen, Jianmin Bao, Shaozhe Hao, Lu Yuan, and Kwan-
 648 Yee K Wong. Uni-ControlNet: All-in-one control to text-to-image diffusion models. *NeurIPS*, 36:
 649 11127–11150, 2023.

648
649
APPENDIX
650
651652
653
A LIMITATIONS
654
655
656
657658
659
First, similar to TokenVerse (Garibi et al., 2025), our method may fail when two customized concepts
660
661 have the same name in the prompt—for example, generating an image based on a prompt where the
662 word “dog” appears twice. Second, when personalizing more than three concepts simultaneously, our
663 method tends to deviate from the concept conditions. We leave addressing these limitations as future
664 work.
665666
667
B MORE RELATED WORKS
668
669670
671
Adapter. Adapters offer an efficient paradigm for customized generation. Several adapter-based
672 methods (Zhang et al., 2023; Mou et al., 2024; Ye et al., 2023; Zhao et al., 2023; Li et al., 2024; Huang
673 et al., 2025) employ lightweight modules for task-specific adaptation while keeping the foundation
674 model weights frozen. For example, ControlNet (Zhang et al., 2023) proposed a trainable copy module
675 of its U-Net-encoder to incorporate spatial control conditions (e.g., edge maps). IP-adapter (Ye et al.,
676 2023) proposed a decoupled cross-attention module to enable the image prompt control. Based on
677 it, MIP-Adapter (Huang et al., 2025) further introduces a weighted-merge mechanism to alleviate
678 the subject confusion problem in multi-subject personalized generation. In this paper, we propose a
679 modulation space adapter module, Mod-Adapter, to predict concept-specific modulation directions
680 while keeping the parameters of the pre-trained DiT backbone frozen.
681682
683
C MORE IMPLEMENTATION DETAILS
684685
686
We use Qwen2.5-VL-7B-Instruct (Team, 2025) as the vision-language model (VLM) for attribute
687 caption and image caption. We train the model using the AdamW (Kingma & Ba, 2014) optimizer
688 with a learning rate of 1×10^{-4} on 8 A800 GPUs. Mod-Adapter is first pre-trained for 50K steps with
689 a batch size of 32 without being integrated into the DiT model, followed by an additional 126K steps
690 of further training with a batch size of 1. Our method has the advantage of supporting multi-concept
691 personalization at inference time while training only on single-concept data, especially given the
692 difficulty of obtaining high-quality multi-concept training data. This ability stems from the localized
693 and composable nature of the DiT modulation space. The scale factor s in Eq. 2 is set to 1 during
694 training and testing. We commit to releasing the source code of our method upon paper acceptance.
695696
697
D USER STUDY DETAILS
698699
700
Fig. 5 shows the user study interface for evaluating single- (a) and multi-concept (b) personalization.
701 To assess concept preservation, participants were asked to rate the similarity between each generated
702 concept and the corresponding concept in the reference image. For multi-concept cases, each concept
703 was evaluated separately, and the final score was calculated by averaging the scores across all concepts.
704 Participants selected from five options, each corresponding to a score from 1 to 5: “Very inconsistent”
705 (1), “Somewhat inconsistent” (2), “Fair” (3), “Quite consistent” (4), and “Very consistent” (5). To
706 assess prompt fidelity, participants evaluated how well the content of the generated image matched
707 the given text prompt, using the same five-point scale.
708709
710
E BROADER IMPACTS
711712
713
The development of the proposed versatile multi-concept personalization generation technique holds
714 potential for broad societal benefits, such as facilitating personalized image creation, storytelling,
715 poster design, and other creative applications. However, this technology may also raise concerns
716 about potential negative societal impacts, such as its misuse to generate misleading or deceptive
717 content, or enabling style-specific personalization that may infringe upon artists’ rights. These risks
718 can be mitigated through techniques such as watermarking generated images and developing robust
719 detection algorithms for content authentication.
720

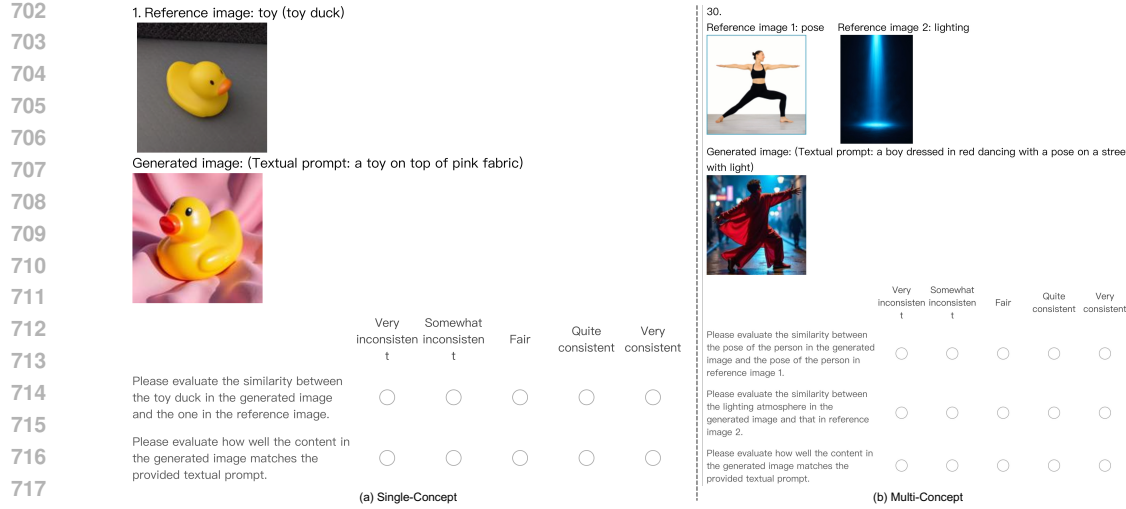


Figure 5: **Screenshot of our user study rating interface.** (a) Single-concept personalization evaluation. (b) Multi-concept personalization evaluation.

Table 4: More quantitative ablation results.

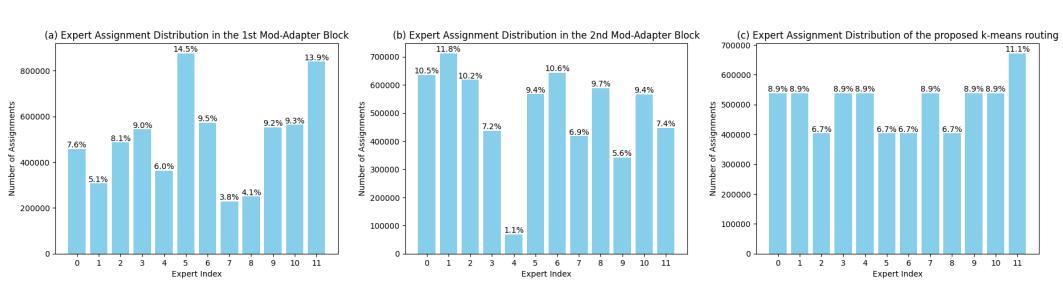
Methods	Multi-concept				single-concept			
	CP	PF	CP-PF	CLIP-T	CP	PF	CP-PF	CLIP-T
Ours (N_expert=1)	0.40	0.54	0.22	0.272	0.36	0.48	0.17	0.278
Ours (N_expert=4)	0.43	0.59	0.25	0.305	0.40	0.78	0.31	0.310
Ours (N_expert=8)	0.57	0.65	0.37	0.310	0.50	0.79	0.40	0.308
Ours (N_expert=12)	0.70	0.89	0.62	0.330	0.61	0.89	0.54	0.315
Hierarchical Clustering (N_expert=12)	0.72	0.88	0.63	0.331	0.62	0.87	0.54	0.313

F MORE ABLATION ANALYSIS

The number of experts and the clustering method. In our MoE routing design, we suspect that concepts within the same cluster may share similar mapping patterns and should therefore be handled by the same expert. Based on this assumption, we set the number of clusters equal to the number of experts, such that each expert is responsible for processing concepts of multiple categories within one cluster. This design choice is empirically validated by our ablation study. Besides, we conducted experiments to investigate the impact of the number of clusters/experts (N_experts) and the choice of clustering method (k-means vs. hierarchical clustering). The results are shown in Tab.4. As observed, increasing the number of experts (i.e., the number of clusters) leads to improved model performance. We used 12 experts in our setup, the maximum that could be accommodated simultaneously within the 80GB GPU memory constraint. To accommodate more experts, the CPU offloading technique can be adopted at the cost of additional offloading overhead. Additionally, the choice between hierarchical and k-means clustering has negligible impact on performance.

K-means MoE Routing. In the ablation study, we design a variant that employs a learnable linear gating network for MoE routing. This variant exhibits suboptimal performance, possibly due to the under-utilization of certain experts. We further analyze the expert utilization pattern in this section and observe that several experts are underused, which is equivalent to using fewer experts than our full model. We visualize the expert assignment patterns of the MoE layers in the 1st and 2nd blocks of Mod-Adapter during training in Fig.6 (a) and Fig.6 (b), respectively. The training set contains 106,104 samples, and for each sample, Mod-Adapter predicts $N = 57$ modulation directions, resulting in 6,047,928 total inputs ($106,104 \times 57$) to each MoE layer per training epoch. Each bar in Fig.6 indicates the percentage of inputs routed to each expert. As shown, Expert 7 (3.8%) and Expert 8 (4.1%) in the first Mod-Adapter block, as well as Expert 4 (1.1%) in the second block, receive significantly fewer inputs during training. This may lead to slower training of these experts, which in turn makes them less likely to be selected in subsequent iterations, resulting in their insufficient

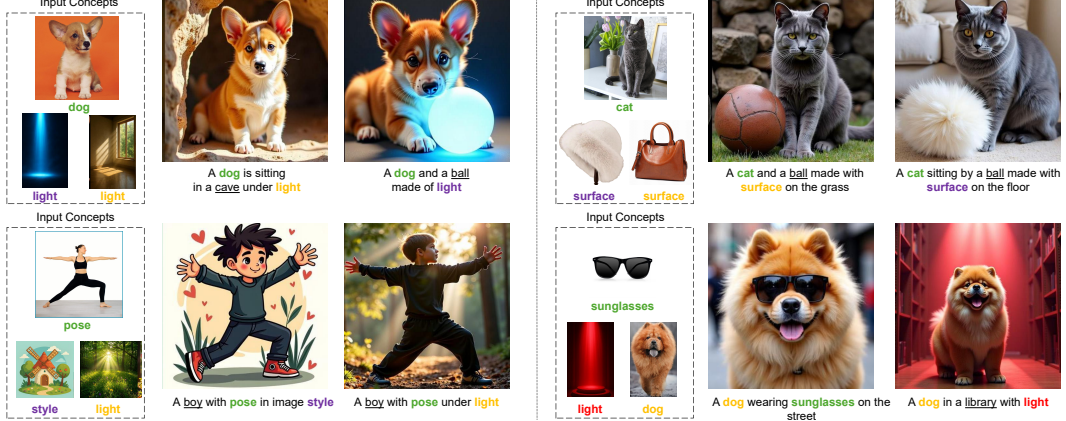
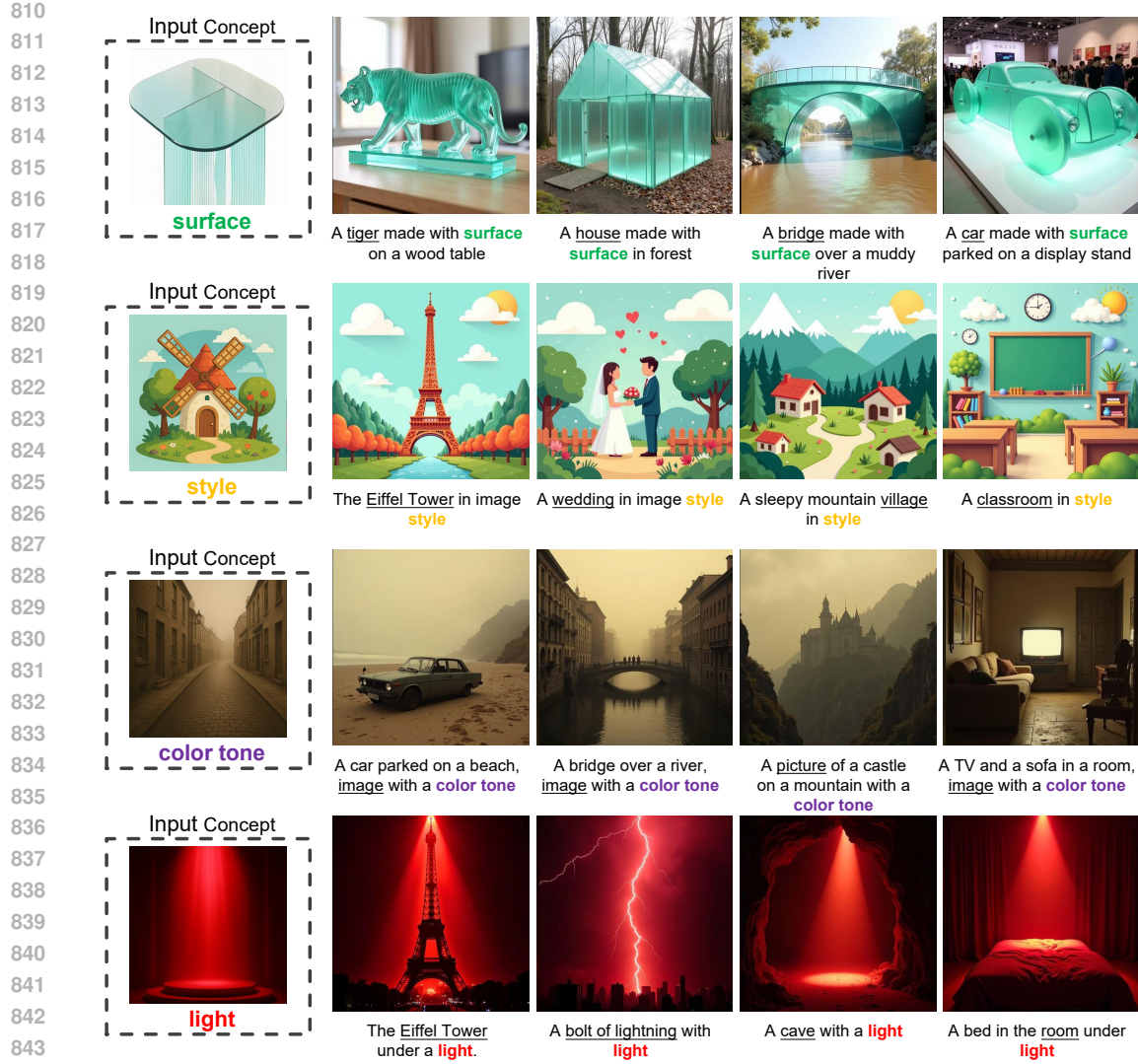
756 utilization. In contrast, our parameter-free k -means-based routing mechanism pre-defines expert
 757 assignments before training, based on k -means clustering over the neutral features of all concept
 758 words in the training dataset, helping ensure sufficient utilization of all experts throughout the training
 759 process as shown in Fig.6 (c).



760
 761 Figure 6: **Distribution of Expert Assignment.** Each bar indicates the percentage of inputs routed to
 762
 763 each expert.
 764
 765
 766
 767
 768

769 G ADDITIONAL QUALITATIVE RESULTS

770 In this section, we present additional qualitative results of our method (see Fig. 7 and Fig. 8).
 771
 772
 773
 774
 775
 776
 777
 778
 779
 780
 781
 782
 783
 784
 785
 786
 787
 788
 789
 790
 791
 792
 793
 794
 795
 796
 797
 798
 799
 800
 801
 802
 803
 804
 805
 806
 807
 808
 809



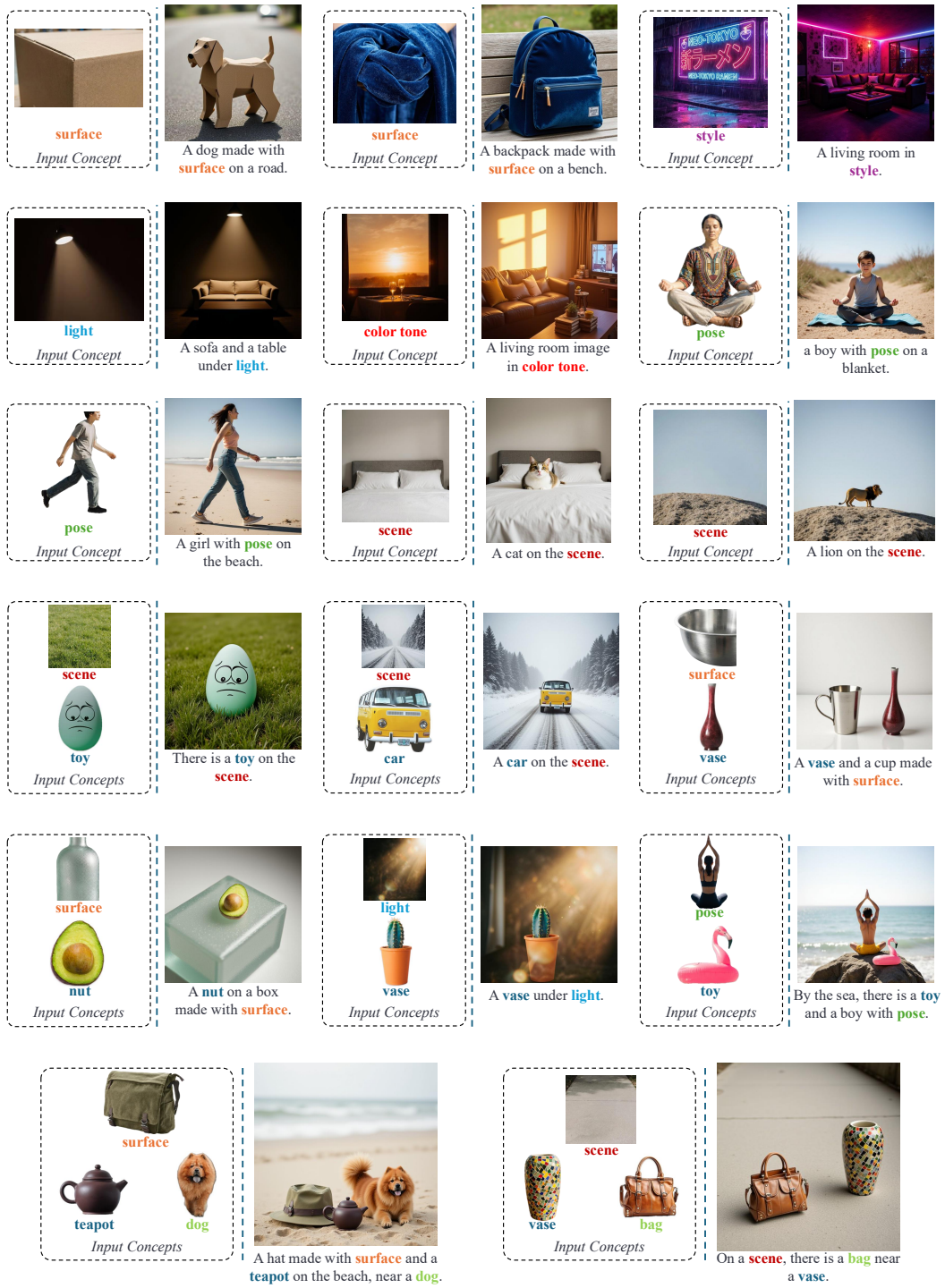
864 **H QUALITATIVE RESULTS FOR THE REBUTTAL**
865

Figure 9: **More qualitative examples of our method on abstract concept personalization.** Colored words in the prompt indicate concepts to be personalized, including abstract concepts and their combinations with object concepts.

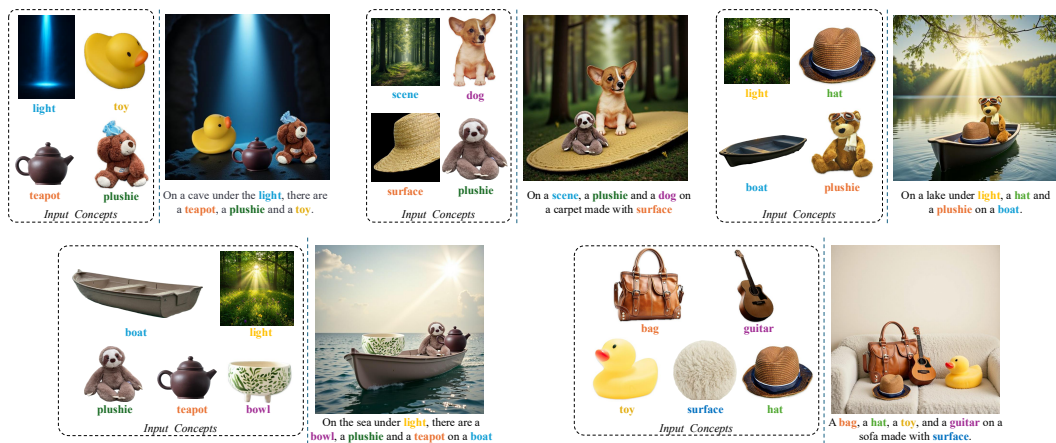


Figure 10: **The qualitative results of our method for customizing an extreme number of concepts (4 to 5 concepts).** Colored words in the prompt indicate concepts to be personalized.



Figure 11: **Qualitative results of combining abstract concepts and concrete objects.** Our method effectively decouples abstract concepts and concrete objects and successfully recombines them. Colored words in the prompt indicate concepts to be personalized.

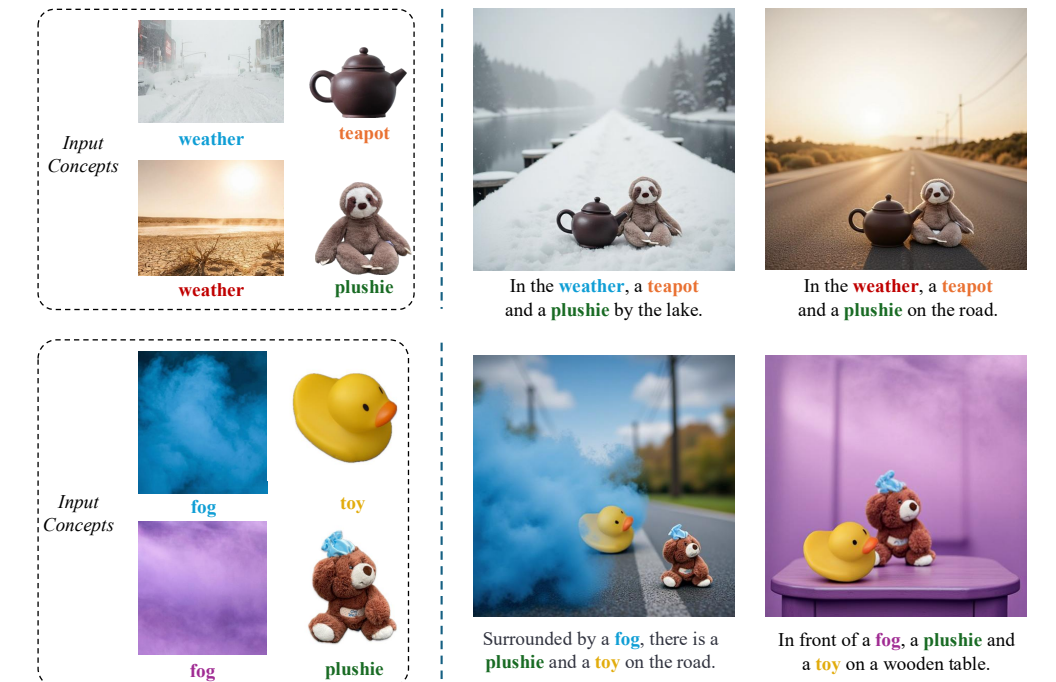


Figure 12: **Qualitative results demonstrating the generalization of our method to concept categories completely unseen during training.** Colored words in the prompt indicate concepts to be personalized.